

Original Article

17-AAG and cisplatin induce structural changes in the diaphragm and regulation of Hsp90, VEGF-C, LYVE-1 expression in a mouse model of malignant ascites

Shijie Cui^{1*}, Yaxin Shen^{2*}, Lei Zhang¹, Qianyu Guo¹, Yanan Zhang¹, Suxia Shao¹, Wei Chen¹, Qing Yin¹, Huijuan Wang¹

Departments of ¹Histology and Embryology, ²Surgical Pandect, Hebei Medical University, Shijiazhuang, Hebei Province, China. *Equal contributors.

Received November 1, 2015; Accepted January 5, 2016; Epub February 1, 2016; Published February 15, 2016

Abstract: Malignant ascites is often caused by metastasis of abdominal tumors. We established a model hepatocellular carcinoma metastasis in 64 mice by injection of 5×10^6 hepatoma H22 cells at six weeks of age. These mice were divided equally into four groups and 24 hours after inoculation were administered with saline, 20 mg/kg 17-AAG, 4 mg/kg Cisplatin, or both 17-AAG and Cisplatin, respectively. Ascites was observed after 10 days in mice administered with saline and the structure of the diaphragm was assessed after 10 days in all animals by histology and scanning and transmission electron microscopy. Expression of heat shock protein 90 (Hsp90), vascular endothelial growth factor-C (VEGF-C), and lymphatic vessel endothelial hyaluronan receptor 1 (LYVE-1) in the diaphragm was assessed by immunohistochemistry, RT-PCR and immunoblotting. In comparison to diaphragm tissues collected from control animals, those collected from model animals revealed disordered cellular arrangement and tumor cells attached to the surface of the diaphragm. These changes were ameliorated by administration of 17-AAG and/or Cisplatin. RT-PCR and immunoblotting revealed that the level of Hsp90, LYVE-1 and VEGF-C mRNA and protein in the diaphragm of tumor-bearing mice was significantly higher than those in healthy control animals ($P < 0.01$). Elevated levels of VEGF-C mRNA and Hsp90 protein were significantly ameliorated by administration of 17-AAG or Cisplatin ($P < 0.05$), and administration of 17-AAG and Cisplatin in combination further reduced the level of these proteins in comparison to either of these drugs alone ($P < 0.05$). These observations suggest 17-AAG can reduce lymphatic metastasis and lymphatic vessel proliferation in diaphragm of mice with malignant ascites.

Keywords: Ascites, metastasis, diaphragm, carcinoma, hepatocellular, vascular endothelial growth factor C

Introduction

Malignant ascites is a common complication of a variety of abdominal carcinomas, accounting for about 10% of all cases of ascites seen in the clinic [1-3]. Malignancies have been reported to cause ascites via a variety of mechanisms. Metastases can obstruct hepatic veins, causing portal hypertension and causing accumulation of fluid in the abdominal cavity [4-8]. Alternatively, accumulation of tumor cells on the peritoneal surface can impair venous and lymphatic drainage [9].

In malignant ascites the peritoneal fluid contains high levels of cells and protein [1], indicating an alteration in vascular permeability. Vessels of the peritoneal lining of experimental

animals with malignant ascites have enhanced permeability [9], and when cell-free malignant ascites fluid was transferred into the intraperitoneal space of healthy control animals, edema was observed, indicating that a soluble factor alters vessel permeability and promotes the formation of malignant ascites [10], likely vascular permeability factor (VEGF) [11].

Lymphatic vessels of the diaphragm drain peritoneal fluid [12], and may represent a method of metastatic tumor cell transportation. The diaphragm pleura is reported to contain openings (peritoneal lymphatic stomata) of the peritoneal lymphatic capillaries among the mesothelial cells of the peritoneum, that serve as the main route for material absorption in the peritoneal cavity [13]. Oya *et al.* injected India ink into

17-aag and cisplatin induce structural changes

monkey peritoneal cavity and found the carbon particles passed through the peritoneal stomata and then the macula cribriformis, ultimately to enter the lymphatic capillaries [14]. Shimada *et al.* found that the macula cribriformis was located between peritoneal mesothelial cells with stomata and subperitoneal lymphatic capillaries. Intraperitoneally-injected latex particles were carried into the diaphragm lymphatic capillaries via the peritoneal stomata and the foramina of the macula cribriformis [15]. In the diaphragm peritoneum, not only tumor cells, but also macrophages and erythrocytes [14, 15] could pass via the peritoneal stomata and the macula cribriformis into the lymphatic lacunae.

Peritoneal lymphatic stomata are associated with ascites absorption [16], and failure of ultrafiltration during cancer metastasis [17]. The peritoneum is covered with a continuous layer of mesothelial cells, and Tsilibary and Wissig confirmed the existence of peritoneal lymphatic stomata by electron microscopy [18]. Further Li *et al.* found the peritoneal lymphatic stomata to be involved in the regulation of pathophysiological activities in the peritoneal cavity [13].

VEGF-C is a potent regulator of lymphatic vessel formation, inducing proliferation of lymphatic endothelial cells *in vitro* and lymphatic hyperplasia *in vivo* [19, 20]. VEGF-C was found to be synthesized by tumor cells that metastasize to lymph nodes, and is considered a specific marker for tumor lymphatic vessels [21-23]. Expression of VEGF has been implicated in generation of malignant ascites [4, 24]. Lymphatic vessel endothelial hyaluronan receptor 1 (LYVE-1) is another marker of lymphatic vessels, expressed specifically on the basal surface of the lymphatic endothelium [25, 26]. LYVE-1 transports hyaluronic acid from the surrounding tissue through lymphatic endothelial cells into the lymphatic system. Using LYVE-1 as a lymphatic marker, studies in mice demonstrated that the production of VEGF-C by tumor cells promoted lymph angiogenesis and subsequent metastasis to the draining lymph nodes [27].

We established a mouse model of hepatocellular carcinoma metastasis in which to investigate how tumor cells in ascites affect the structure and function of the diaphragm. We found that hepatocellular carcinoma cells attached to the diaphragm and induced structural changes

associated with increased expression of VEGF-C and LYVE-1.

Allylamino-17-demethoxygeldanamycin (17-AAG) is an inhibitor of Hsp90 Heat shock proteins, which are chaperones of the folding of many oncogenic proteins, and crucial for the proliferation and survival of many cancers [28]. 17-AAG showed some promise as an anti-cancer therapeutic in the clinic [29]. Administration of chemotherapeutic agents 17-AAG and cisplatin ameliorated the pathological changes observed in the diaphragm.

Materials and methods

Cell culture

The Hepatoma cell line H22 was obtained from Type 131 Culture Collection of Chinese Academy of Sciences, and cultured in RPMI 1640 supplemented with 2 mM l-glutamine (Sigma, St Louis, MO), 100 IU/ml penicillin and 100 nM Od streptomycin (Life Technologies, Paisley, UK), and 10% fetal bovine serum (Gibco, Grand Island, NY) at 37 °C under humidified conditions with 5% CO₂.

Animals

Forty male and forty female BALB/c mice, 6-8 weeks old, weighing 18-22 g, were procured from the Experimental Animal Center of Hebei Medical University (Shijiazhuang, China) and housed in polycarbonate cages with filter tops. Animals were provided with food and water ad libitum, and treated in compliance with the Principles of Laboratory Animal Care formulated by the National Society for Medical Research and the Guide for the Care and Use of Laboratory Animals prepared by the National Academy of Sciences (National Institutes of Health Publication No. 80-23, revised 1978). Animals were housed at 25±2 °C, with 50±2% relative humidity and a photoperiod of 12 h throughout the study.

Animal inoculation and treatment

Mice were randomly divided into five groups of 16. One group of control animals (CON group) received intraperitoneal injection of physiologic saline. Mice in the other 4 groups received intraperitoneal injection of Hepatoma H22 cell (1×10⁷ cells/ml, 0.5 ml/mouse) in order to establish a model of ascites. 24 hours after inoc-

17-aag and cisplatin induce structural changes

ulation, 16 mice received injections of Hsp90 inhibitor 17-AAG (20 mg/kg) once every two days (AAG group). 16 mice received injections of 4 mg/kg cisplatin once every two days (CIS group), and 16 mice received injections of 20 mg/kg 17-AAG and 4 mg/kg cisplatin once every two days, all for 10 days (COM group).

After 10 days mice were sacrificed by ether. In each group half the male and half the female mice were used for histopathological studies, the remaining animals for biochemical studies.

HE staining

Mice anesthetized by ether were perfused with 4% paraformaldehyde, and the intact diaphragms were immediately further fixed with 4% paraformaldehyde for 24 hours, and embedded in paraffin, sectioned at 4 μ m, stained with hematoxylin and eosin (HE) and observed under a light microscope.

Scanning electronic microscopy (SEM)

After perfusion and post-fixation, the diaphragms were then rinsed in PBS for 5 min for 3 times. The samples were treated with 1% Tannin at room temperature (RT) for 30 min, and then rinsed. The samples were fixed for 1 hour in 1% osmic acid (0.2 M PBS: 2% osmic acid 1:1), and then rinsed. Samples were dehydrated in a graded series of ethanol solutions from 50% to 100% ethanol, and then incubated in a thiobarbituric acid solution for 30 min at 37°C, and at 4°C overnight. Coated tissue samples were fixed on mini-plates with silver glue (Nebauer Chemikalien, Muenster, Germany), and then further coated with a Sputter Coater coating device (Bio-Rad, Wadford, UK). The coated diaphragms were evaluated with an S-3500N SEM (Hitachi, Japan). Five sections of the parietal surface of the peritoneum were examined at magnifications of $\times 100$ to $\times 5,000$.

Transmission electron microscopy (TEM)

After perfusion and post-fixation, the diaphragms were rinsed in PBS, and fixed in 0.1 mol/l Na-cacodylate buffer containing 2.5% glutaraldehyde in for 2 h at RT. Samples were then submerged in 0.1 M PBS containing 0.1% osmic acid for 1 h at 4°C, and dehydrated in a graded series of 40% to 100% ethanol, then propylene oxide and embedded in epoxy-resin. Embedded samples were sectioned into 400-500 nm slices with a Reichert Jounq Ultracut-E ultramicro-

tome (Heidelberg, Germany), and the sections were stained with uranyl acetate and lead citrate, and observed under an EM-109 Zeiss transmission electron microscope (Jena, Germany).

Immunohistochemical staining

After perfusion and post-fixation, the diaphragm sections (4 μ m) were mounted on poly-L-lysine-coated slides, and slides were deparaffinized in xylene. Endogenous peroxidase activity was blocked with 3% hydrogen peroxide in 50% methanol for 10 min at RT. Sections were rehydrated in alcohol, washed with PBS, and pretreated with 0.01 M citric acid (pH 6.0) for 20 min in a 95°C water bath. After blocking with 10% normal goat serum in PBS for 20 min at 37°C, the sections were incubated overnight at 4°C with rabbit polyclonal anti-mouse Hsp90 (Bioworld Technology, Nanjing, China), rabbit polyclonal anti-actin (Zhongshan Golden Bridge Biotechnology, Beijing, China), rabbit polyclonal anti-LYVE-1 (Bioworld Technology), rabbit polyclonal anti-VEGFC (Cell Signaling Technologies, Danvers, MA). After incubation, the sections were rinsed with PBS, incubated with biotinylated goat anti-rabbit IgG (Zhongshan Golden Bridge Biotechnology) for 30 min at 37°C, then incubated with 3,3'-diaminobenzidine chromogen (Zhongshan Golden Bridge Biotechnology) for 5 to 10 min at RT and washed with distilled water. Finally, the sections were counterstained with hematoxylin for 1 min followed by dehydration and mounting. Sections used as negative control were incubated with PBS only without the primary antibodies.

Quantitative RT-PCR

The level of Hsp90, LYVE-1 and VEGFC mRNA in mouse diaphragms was quantized using the ABI Fast quantitative PCR 7900HT system (Applied Biosystems, Grand Island, NY). Briefly, total RNA was extracted using Trizol (Invitrogen) according to the manufacturer's protocol and cDNA was prepared with 3 μ g total RNA using the reverse transcription system (Promega, Madison, WI). Equal amounts of cDNA were subjected to PCR, in the presence of SYBR green dye with the Platinum SYBR Green qPCR SuperMix-UDG kit (Invitrogen) and the PCR without template was used as a negative control. β -actin mRNA was used as an internal control. Hsp90, LYVE-1, VEGFC and β -actin mRNA were amplified on the same plate. Target gene and

17-aag and cisplatin induce structural changes

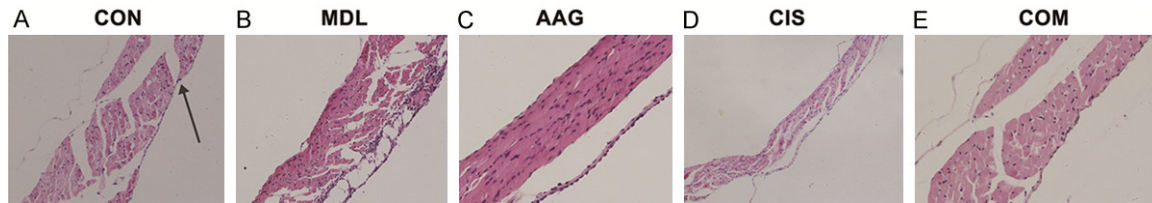


Figure 1. HE staining of the diaphragm in a mouse model of HCC metastasis-induced ascites. The diaphragms of healthy 8 weeks old BALB/c mice were isolated and subjected to H&E staining. The epithelial cells of the diaphragm were closely and regularly arranged with oval nuclei. The lymph-vessel is filled with black ink and the blood vessel is filled with blood (CON group). In mice that received injection of 1×10^6 Hepatoma H22 cells at six weeks of age, ascites was observed after 10 days and in diaphragms cellular arrangement was disordered. Epithelial cells were cubic with enlarged nuclei and tumor cells were found attached to the surface of the diaphragm. Connective tissue hyperplasia, and irregular lumens were also observed beneath the epithelial layer, and tumor cells had infiltrated through the lumen (MDL group). In mice that received injection of 20 mg/kg 17-AAG (AAG group) or 4 mg/kg cisplatin (CIS group) 24 h after H22 cell injection, the diaphragms appeared to be healthier than those of the MDL group. In mice that received both 17-AAG and cisplatin the diaphragms were indistinguishable from healthy control animals (COM group). All images (200 \times) are representative images of 3 different experiments.

β -actin specific primers were designed using the Primer Premier 5 software as follows: Hsp90 sense: 5'-TATTCTGCCTTCCTTGTA-3', anti-sense: 5'-GTGTGTTTTCTCTTGGGT-3'; 124 bp; LYVE-1 sense: 5'-AGGAGCCCTCCTTACTGC-3', anti-sense: 5'-ACCTGGAAGCCTGTCTCTGA-3'; 174 bp; VEGF-C sense: 5'-CAGTGTCAGGCAGC-TAACAAAG-3', anti-sense: 5'-GGTCCACAGACATC-ATGGAA-3'; 143 bp; β -actin sense: 5'-AACAGT-CCGCCTAGAAGCAC-3', anti-sense: 5'-CGTTGA-CATCCGTAAGACC-3'.

PCR was performed in 40 cycles of 5 s at 95 $^{\circ}$ C, 20 s at 60 $^{\circ}$ C and 20 s at 72 $^{\circ}$ C after a 30 s initial denaturation at 95 $^{\circ}$ C. Each sample was normalized by using the difference in critical thresholds (CT) between target gene and β -actin. The following equation was used to describe the result: $\Delta Th_{\text{target gene}} = \Delta CT_{\text{target gene}} - \Delta CT_{\beta\text{actin}}$. The mRNA levels of each sample were then compared using the expression $2^{-\Delta\Delta CT}$.

Immunoblotting

To examine level of Hsp90, LYVE-1 and VEGFC in the diaphragm, isolated tissue samples were washed twice with cold PBS and lysed on ice in RIPA lysis buffer (50 mM Tris, 150 mM NaCl, 1% Triton X-100, 1 mM EDTA, pH 7.5) with HaltTM protease & phosphatase inhibitor cocktail (Thermo, Rockford, IL) for 30 min. The suspension was centrifuged for 10 min at 4,000 g at 4 $^{\circ}$ C, and the protein concentration of supernatants was determined with a BCA kit (Pierce, Rockford, IL). The loading buffer containing 100 mM Tris/HCl (pH 6.8), 4% SDS, 20% glycerin, 10% ktamercaptoethanol and 0.2% bromophenol blue was added, and samples were then

denatured at 95 $^{\circ}$ C for 10 min. 20 μ g of protein was loaded in each well and separated in 10% SDS polyacrylamide electrophoresis gels. The proteins were transferred onto nitrocellulose membranes (Bio-Rad, Hercules, CA). The membranes were blocked with 5% fat-free milk at 37 $^{\circ}$ C for 1 h, and incubated with rabbit polyclonal rabbit anti-Hsp90, LYVE-1, VEGF-C (Santa Cruz Biotechnology, Dallas, Texas) for 2 h at 37 $^{\circ}$ C. After thorough washing, the sections were incubated with goat anti-rabbit HRP and goat anti-mouse HRP (Pierce), respectively, for 45 min followed by extensive washes (1-2 h). Specific antibody-antigen complexes were detected using the ECL Western blot detection kit (Pierce). The extent of blot staining was recorded in the linear range of detection and quantified to indicate the level of specific induction by scanning laser densitometry. Protein expression was quantified by densitometry with Gel pro 3.0 image software (Media Cybernetics, Silver-spring, MD).

Statistical analysis

Data were expressed as mean \pm SD and ANOVA analyses were performed using SPSS 13.0 statistical software.

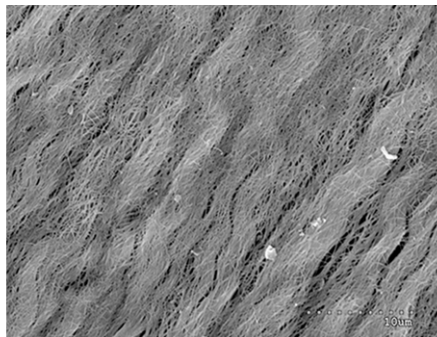
Results

HCC metastasis induces anatomical changes in diaphragm structure

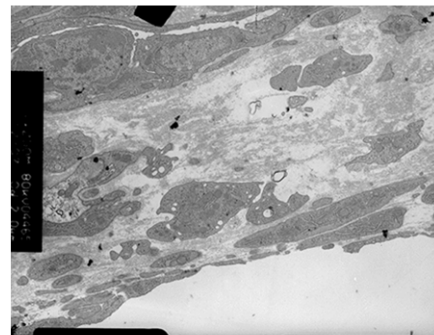
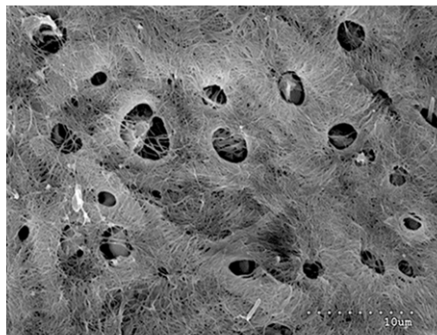
A mouse model of HCC metastasis-induced ascites was established by injection of 5×10^6 hepatoma H22 cells into the peritoneal cavities of mice. Within seven days ascites was observed. The abdomen of mice was swollen, and

17-aag and cisplatin induce structural changes

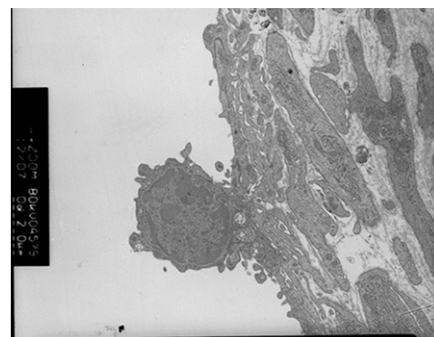
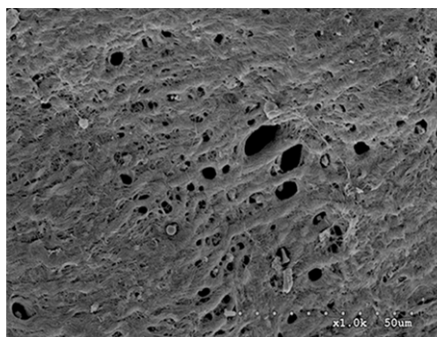
CON group



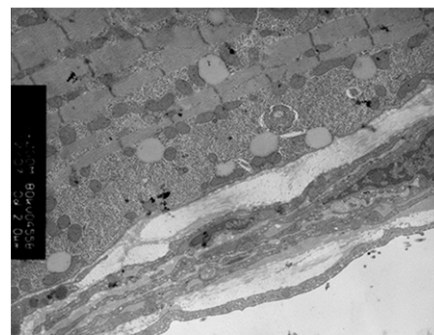
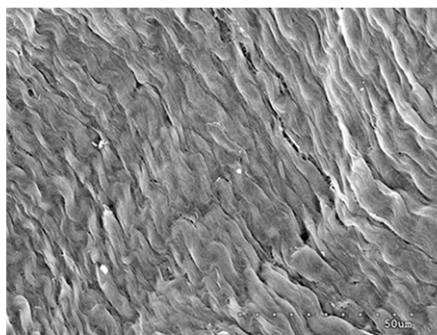
MDL group



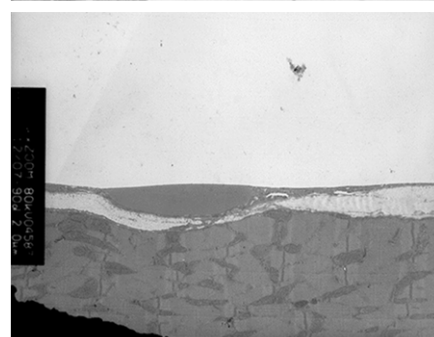
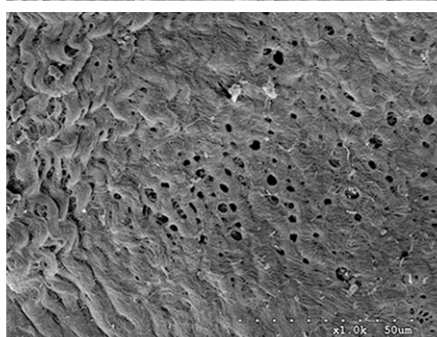
AAG group



CIS group



COM group



17-aag and cisplatin induce structural changes

Figure 2. Scanning and transmission electron microscopy reveal the ultrastructure of the diaphragm in a mouse model of malignant ascites. The diaphragms of healthy 8 weeks old BALB/c mice were isolated and subjected to Scanning electron microscopy, SEM ($\times 1000$) and transmission electron microscopy, TEM ($\times 5000$) (CON group). In mice that received injection of 1×10^6 Hepatoma H22 cells at six weeks of age (MDL group), cells were irregularly arranged, increased hyperplasia of connective tissue was observed, and tumor cells were attached to the surface of the diaphragm. Cribriporals were more prevalent and increased in diameter. In mice that received injection of 20 mg/kg 17-AAG (AAG group), or 4 mg/kg cisplatin (CIS group) or both (COM group) 24 h after H22 cell injection, the diaphragms resembled those in the CON group. Images are representative of 2 different experiments.

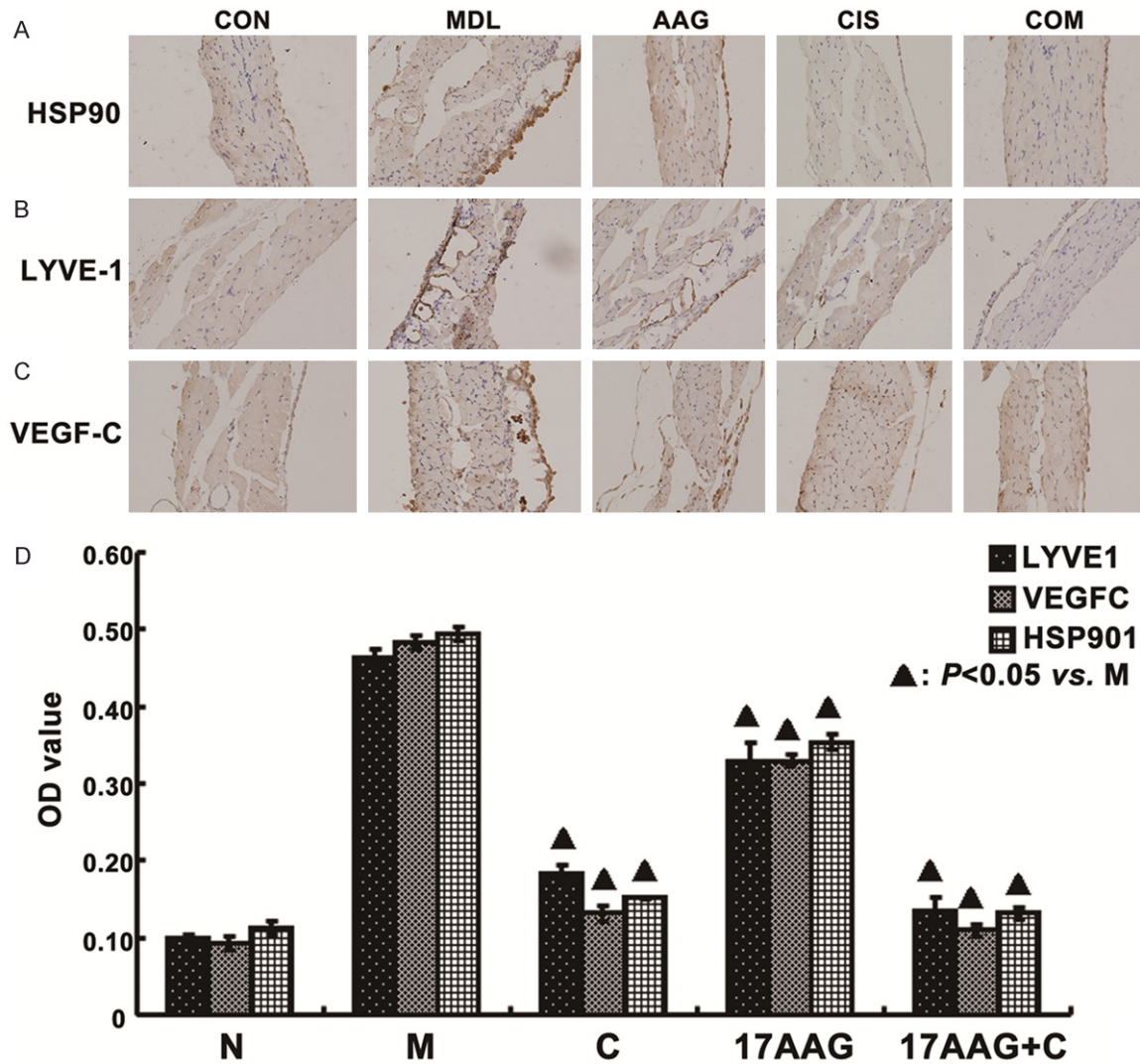


Figure 3. Hsp90, Lyve-1 and Vegfc protein distribution in the diaphragms in a mouse model of malignant ascites. The diaphragms of healthy 8 weeks old BALB/c mice were isolated and subjected to immunostaining for Hsp90 (A), LYVE-1 (B) and VEGFC (C). The brown color indicates positive staining. All images ($200\times$) are representative images of 3 different experiments. Staining density was quantified (D). N, control animals (CON); M, model animals (MDL); C, animals administered Cisplatin (CIS); 17AAG, animals administered 17AAG (AAG); 17AAG + C, animals administered 17AAG + Cisplatin (COM).

appetite, weight, activity, and response to stimuli were reduced. Whilst tissues collected from control animals revealed that the epithelial cells of the diaphragm were closely and regu-

larly arranged with oval nuclei (**Figure 1A**), the cellular arrangement of the diaphragms of mice administered H22 cells was disordered. Epithelial cells were cubic with enlarged nuclei and

17-aag and cisplatin induce structural changes

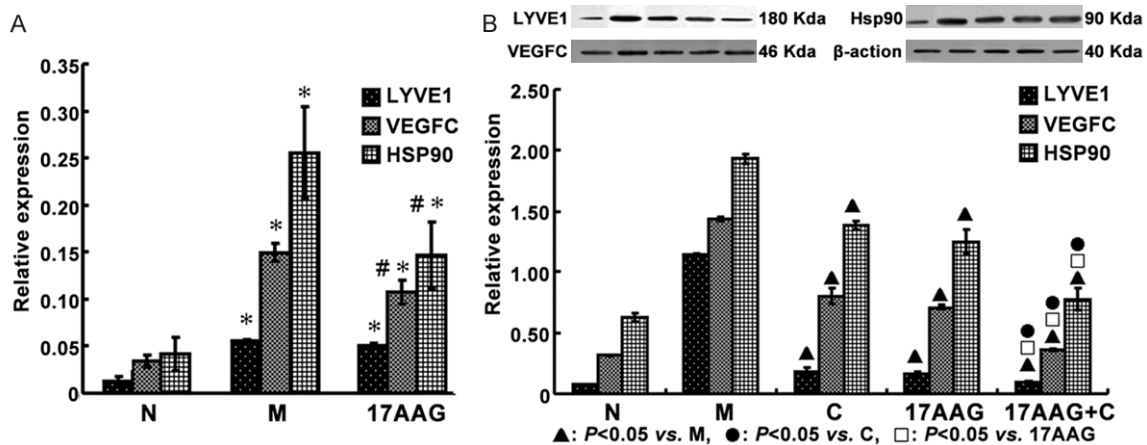


Figure 4. Hsp90, LYVE-1 and VEGF-C mRNA and protein content of the diaphragm in a mouse model of malignant ascites. The diaphragms of healthy 8 week old BALB/c mice were isolated and the level of Hsp90, LYVE-1 and VEGF-C mRNA and protein was assessed by RT-PCR (A) and immunoblotting (B). For RT-PCR β -actin was used as an internal control. In comparison to healthy control animals, the level of Hsp90, LYVE-1 and VEGF-C mRNA was higher in mice administered 1×10^6 Hepatoma H22 cells at six weeks of age ($*P < 0.05$), however these elevated levels of VEGF-C and Hsp90 mRNA were significantly ameliorated by administration of 17-AAG ($\#P < 0.05$). In comparison to healthy control animals, the level of Hsp90, LYVE-1 and VEGF-C protein were higher in mice administered 1×10^6 Hepatoma H22 cells at six weeks of age ($*P < 0.05$), however the elevated levels of all three proteins were significantly ameliorated by administration of 17-AAG or Cisplatin ($P < 0.05$), and administration of 17-AAG and Cisplatin in combination further reduced the level of these proteins in comparison to either of these drugs alone ($P < 0.05$). Data represent 3 independent experiments with SD. N, control animals; M, model animals; C, animals administered Cisplatin; 17AAG, animals administered 17AAG; 17AAG + C, animals administered 17AAG + Cisplatin.

tumor cells were found attached to the surface of the diaphragm. Connective tissue hyperplasia, and irregular lumens were also observed beneath the epithelial layer, and tumor cells were observed to have infiltrated through the lumen (Figure 1B). In mice which received 20 mg/kg Hsp90 inhibitor 17-AAG or 4 mg/kg cisplatin 24 hours following infusion of H22 cells, then every two days for 10 days (AAG and CIS group, respectively) (Figure 1C and 1D, respectively), the cellular arrangement of the diaphragms were observed to be much better than that in MDL groups. In mice which received both 17-AAG and cisplatin (COM group), the diaphragms were indistinguishable from healthy control animals (Figure 1E).

SEM and TEM of diaphragm tissues confirmed the results of histological analysis (Figure 2). In the diaphragms of MDL group mice diaphragm muscle mesothelial cells were irregularly arranged, increased hyperplasia of connective tissue was observed, and tumor cells were found to be attached to the surface of the diaphragm. Cribriporals were more prevalent and increased in diameter. In the AAG, CIS and COM groups, the mesothelial cells resembled those seen in healthy control animals (Figure 2).

Diaphragm cell expression of Hsp90, LYVE-1 and VEGF-C were upregulated in a mouse model of malignant ascites, but ameliorated by administration of 17-AAG and/or cisplatin

The level of Hsp90, LYVE-1 and VEGFC expression in diaphragms was assessed by immunohistochemical staining (Figure 3). In comparison to the mice in CON group, increased levels of Hsp90 and VEGF-C were observed in specimens from MDL group mice (Figure 3). LYVE-1-positive lymphatic vessels were observed in the diaphragms of mice in each group. LYVE-1 expression was lower in the normal lymphatic endothelial cells and diaphragm epithelial cells than in specimens from tumor-bearing mice. Strong LYVE-1 staining was observed in the cytoplasm of tumor cells, however LYVE-1 staining was significantly decreased in the tumor cells of mice treated with 17-AAG (Figure 3).

RT-PCR and immunoblotting revealed that the level of Hsp90, LYVE-1 and VEGF-C mRNA and protein in the diaphragm of tumor-bearing mice was significantly higher than that in healthy control animals ($P < 0.01$). However these elevated levels of VEGF-C mRNA and Hsp90 mRNA were significantly ameliorated by administra-

17-aag and cisplatin induce structural changes

tion of 17-AAG ($P < 0.05$). In comparison to healthy control animals, the level of Hsp90, LYVE-1 and VEGF-C protein were higher in tumor-bearing mice ($P < 0.05$), however these elevated levels of all three proteins were significantly ameliorated by administration of 17-AAG or Cisplatin ($P < 0.05$), and administration of 17-AAG and Cisplatin in combination further reduced the level of these proteins in comparison to either of these drugs alone ($P < 0.05$) (**Figure 4**).

Discussion

In order to investigate the role of the diaphragm in malignant ascites, we established a mouse model of hepatocellular carcinoma metastasis. We found numerous stomata in the diaphragm pleura, anterior costal pleura and the mediastinal pleura in mice. The diaphragm pleura were covered with two different types of mesothelial cells: one small and round and the other large and flat. Macula cribriformis have been observed in the diaphragm pleura of the monkey, rat, and mouse in SEM studies [14, 15]. We found macula cribriformis between the mesothelial cells with stomata and the lymphatic lacunae. Macula cribriformis of the foramina were larger than those of the mesothelial stomata and appeared to correspond to those areas lacking collagen fibers. These results indicated that the foramina of the macula cribriformis also form short channels between the pleural cavity and the lymphatic lacunae or between the pleural mesothelial cells and the lymphatic lacunae. The diaphragm lymphatic vessels are densely distributed and form a multi-layered, crossed network with great absorption functionality. Li *et al.* found that in ascites fluid, granular materials, microbes and cancer cells can enter diaphragm lymphatic vessels through the peritoneal lymphatic stomata [30]. The diaphragm lymphatic vessels represent an important part of the peritoneal lymph system and are the primary route of absorption from the peritoneal cavity [31]. In this study, we observed that tumor cells entered the diaphragm lymphatic vessels through peritoneal lymphatic stomata.

We found that malignant ascites was associated with increased expression of VEGF-C and LYVE-1 mRNA and protein and lymphatic vessel proliferation in the diaphragm. VEGF-C, a key regulator of lymphangiogenesis and angiogenesis has previously been found to be overex-

pressed in cancer tissues [32], and was found to be a more accurate marker of lymph node metastasis than chest computed tomography in non-small cell lung carcinoma [33]. Overexpression of VEGF-C was also associated with pathological features of esophageal squamous cell carcinoma [34] including depth of tumor invasion, cancer stage, lymph node metastasis and lymphatic or venous invasion [34-37]. VEGF-C binds and activates Vascular endothelial growth factor receptor-3 (VEGFR-3) which is mainly expressed on lymphatic endothelial cells, and activation of VEGFR-3 contributes to the expansion of lymphatic vessels in tumors and tumor cell migration to lymphatic vessels [22].

In seminomatous testicular cancer cells increased LYVE-1 levels correlated with increased lymphangiogenesis [38]. LYVE-1 is also expressed in lymphatic endothelial cells and mediates Fibroblast growth factor-2 (FGF2)-positive tumor cell recruitment to lymphatic vessels [39]. Our observations implicate these two molecules in the process by which tumor cells pass through the diaphragm pleura.

We also observed increased levels of Hsp90 in the diaphragms of mice with malignant ascites, and administration of Hsp90 inhibitor 17-AAG restored order to the diaphragm, reducing the size of peritoneal pores, and reduced the levels of VEGF-C, LYVE-1 and Hsp90 detected in the diaphragm. Administration of 17-AAG and Cisplatin in combination further reduced the level of these proteins in comparison to either of these drugs alone. These observations suggest reduced lymph metastasis and lymphatic vessel proliferation in the tumor tissue.

In conclusion, we found that in a mouse model of HCC metastasis, malignant ascites could induce remarkable structural changes in the diaphragm. The epithelial cells were disordered and higher levels of Hsp90, a marker of tumor cells, and VEGF-C and LYVE-1, markers of lymphangiogenesis were detected in the diaphragm. Inhibition of Hsp90 with 17-AAG significantly corrected these pathological changes and reduced expression of LYVE-1 and VEGF-C suggesting that this drug represents a promising therapeutic for the inhibition of lymphatic metastasis.

Disclosure of conflict of interest

None.

17-aag and cisplatin induce structural changes

Address correspondence to: Dr. Lei Zhang, Department of Histology and Embryology, Hebei Medical University, Shijiazhuang, Hebei Province, China. Tel: +86-13903210199; Fax: +86-21-64085875; E-mail: 13903210199@139.com

References

- [1] Runyon BA, Hoefs JC and Morgan TR. Ascitic fluid analysis in malignancy-related ascites. *Hepatology* 1988; 8: 1104-1109.
- [2] Runyon BA. Care of patients with ascites. *N Engl J Med* 1994; 330: 337-342.
- [3] Kashani A, Landaverde C, Medici V and Ros-saro L. Fluid retention in cirrhosis: pathophysiology and management. *QJM* 2008; 101: 71-85.
- [4] Nagy JA, Masse EM, Herzberg KT, Meyers MS, Yeo KT, Yeo TK, Sioussat TM and Dvorak HF. Pathogenesis of ascites tumor growth: vascular permeability factor, vascular hyperpermeability, and ascites fluid accumulation. *Cancer Res* 1995; 55: 360-368.
- [5] Intaglietta M and Zweifach BW. Microcirculatory basis of fluid exchange. *Adv Biol Med Phys* 1974; 15: 111-159.
- [6] Holm-Nielsen P. Pathogenesis of ascites in peritoneal carcinomatosis. *Acta Pathol Microbiol Scand* 1953; 33: 10-21.
- [7] Feldman GB, Knapp RC, Order SE and Hellman S. The role of lymphatic obstruction in the formation of ascites in a murine ovarian carcinoma. *Cancer Res* 1972; 32: 1663-1666.
- [8] Nagy JA, Herzberg KT, Dvorak JM and Dvorak HF. Pathogenesis of malignant ascites formation: initiating events that lead to fluid accumulation. *Cancer Res* 1993; 53: 2631-2643.
- [9] Senger DR, Galli SJ, Dvorak AM, Perruzzi CA, Harvey VS and Dvorak HF. Tumor cells secrete a vascular permeability factor that promotes accumulation of ascites fluid. *Science* 1983; 219: 983-985.
- [10] Garrison RN, Kaelin LD, Galloway RH and Heuser LS. Malignant ascites. Clinical and experimental observations. *Ann Surg* 1986; 203: 644-651.
- [11] Zebrowski BK, Liu W, Ramirez K, Akagi Y, Mills GB and Ellis LM. Markedly elevated levels of vascular endothelial growth factor in malignant ascites. *Ann Surg Oncol* 1999; 6: 373-378.
- [12] Kim KE, Koh YJ, Jeon BH, Jang C, Han J, Kataru RP, Schwendener RA, Kim JM and Koh GY. Role of CD11b+ macrophages in intraperitoneal lipopolysaccharide-induced aberrant lymphangiogenesis and lymphatic function in the diaphragm. *Am J Pathol* 2009; 175: 1733-1745.
- [13] Li JC and Yu SM. Study on the ultrastructure of the peritoneal stomata in humans. *Acta Anat (Basel)* 1991; 141: 26-30.
- [14] Oya M, Shimada T, Nakamura M and Uchida Y. Functional morphology of the lymphatic system in the monkey diaphragm. *Arch Histol Cytol* 1993; 56: 37-47.
- [15] Shimada T, Zhang L and Oya M. Architecture and function of the extravascular fluid pathway: special reference to the macula cribiformis in the diaphragm. *Kaibogaku Zasshi* 1995; 70: 140-155.
- [16] Li J. [Study on the peritoneal stomata and absorptive mechanism of ascites]. *Zhongguo Yi Xue Ke Xue Yuan Xue Bao* 1992; 14: 328-333.
- [17] Funatsu K, Nishihara H, Nozaki Y, Sakai T, Tomoda N, Itoh Y and Hayabuchi N. A case of a solitary metastatic diaphragmatic tumor—relation to the peritoneal stomata of the diaphragm. *Radiat Med* 1998; 16: 363-365.
- [18] Tsilibary EC and Wissig SL. Absorption from the peritoneal cavity: SEM study of the mesothelium covering the peritoneal surface of the muscular portion of the diaphragm. *Am J Anat* 1977; 149: 127-133.
- [19] Oh SJ, Jeltsch MM, Birkenhager R, McCarthy JE, Weich HA, Christ B, Alitalo K and Wilting J. VEGF and VEGF-C: specific induction of angiogenesis and lymphangiogenesis in the differentiated avian chorioallantoic membrane. *Dev Biol* 1997; 188: 96-109.
- [20] Jeltsch M, Kaipainen A, Joukov V, Meng X, Laksso M, Rauvala H, Swartz M, Fukumura D, Jain RK and Alitalo K. Hyperplasia of lymphatic vessels in VEGF-C transgenic mice. *Science* 1997; 276: 1423-1425.
- [21] Breiteneder-Geleff S, Soleiman A, Kowalski H, Horvat R, Amann G, Kriehuber E, Diem K, Weninger W, Tschachler E, Alitalo K and Kerjaschki D. Angiosarcomas express mixed endothelial phenotypes of blood and lymphatic capillaries: podoplanin as a specific marker for lymphatic endothelium. *Am J Pathol* 1999; 154: 385-394.
- [22] Kukk E, Lymboussaki A, Taira S, Kaipainen A, Jeltsch M, Joukov V and Alitalo K. VEGF-C receptor binding and pattern of expression with VEGFR-3 suggests a role in lymphatic vascular development. *Development* 1996; 122: 3829-3837.
- [23] Partanen TA, Alitalo K and Miettinen M. Lack of lymphatic vascular specificity of vascular endothelial growth factor receptor 3 in 185 vascular tumors. *Cancer* 1999; 86: 2406-2412.
- [24] Numnum TM, Rocconi RP, Whitworth J and Barnes MN. The use of bevacizumab to palliate symptomatic ascites in patients with refractory ovarian carcinoma. *Gynecol Oncol* 2006; 102: 425-428.
- [25] Jackson DG. Biology of the lymphatic marker LYVE-1 and applications in research into lymphatic trafficking and lymphangiogenesis. *AP-MIS* 2004; 112: 526-538.

17-aag and cisplatin induce structural changes

- [26] Prevo R, Banerji S, Ferguson DJ, Clasper S and Jackson DG. Mouse LYVE-1 is an endocytic receptor for hyaluronan in lymphatic endothelium. *J Biol Chem* 2001; 276: 19420-19430.
- [27] Jackson DG, Prevo R, Clasper S and Banerji S. LYVE-1, the lymphatic system and tumor lymphangiogenesis. *Trends Immunol* 2001; 22: 317-321.
- [28] Hong DS, Banerji U, Tavana B, George GC, Aaron J and Kurzrock R. Targeting the molecular chaperone heat shock protein 90 (HSP90): lessons learned and future directions. *Cancer Treat Rev* 2013; 39: 375-387.
- [29] Gartner EM, Silverman P, Simon M, Flaherty L, Abrams J, Ivy P and Lorusso PM. A phase II study of 17-allylamino-17-demethoxygeldanamycin in metastatic or locally advanced, unresectable breast cancer. *Breast Cancer Res Treat* 2012; 131: 933-937.
- [30] Li H and Li J. Development of the peritoneal lymphatic stomata and lymphatic vessels of the diaphragm in mice. *Ann Anat* 2003; 185: 411-418.
- [31] Azzali G. The lymphatic vessels and the so-called lymphatic stomata of the diaphragm: a morphologic ultrastructural and three-dimensional study. *Microvasc Res* 1999; 57: 30-43.
- [32] Tammela T, Enholm B, Alitalo K and Paavonen K. The biology of vascular endothelial growth factors. *Cardiovasc Res* 2005; 65: 550-563.
- [33] Tamura M, Oda M, Tsunozuka Y, Matsumoto I, Kawakami K, Ohta Y and Watanabe G. Chest CT and serum vascular endothelial growth factor-C level to diagnose lymph node metastasis in patients with primary non-small cell lung cancer. *Chest* 2004; 126: 342-346.
- [34] Kitadai Y, Amioka T, Haruma K, Tanaka S, Yoshihara M, Sumii K, Matsutani N, Yasui W and Chayama K. Clinicopathological significance of vascular endothelial growth factor (VEGF)-C in human esophageal squamous cell carcinomas. *Int J Cancer* 2001; 93: 662-666.
- [35] Byeon JS, Jung HY, Lee YJ, Lee D, Lee GH, Myung SJ, Yang SK, Hong WS, Kim JH, Min YI and Kim JS. Clinicopathological significance of vascular endothelial growth factor-C and cyclooxygenase-2 in esophageal squamous cell carcinoma. *J Gastroenterol Hepatol* 2004; 19: 648-654.
- [36] Kimura Y, Watanabe M, Ohga T, Saeki H, Kakeji Y, Baba H and Maehara Y. Vascular endothelial growth factor C expression correlates with lymphatic involvement and poor prognosis in patients with esophageal squamous cell carcinoma. *Oncol Rep* 2003; 10: 1747-1751.
- [37] Krzystek-Korpacka M, Matusiewicz M, Diakowska D, Grabowski K, Blachut K and Banas T. Up-regulation of VEGF-C secreted by cancer cells and not VEGF-A correlates with clinical evaluation of lymph node metastasis in esophageal squamous cell carcinoma (ESCC). *Cancer Lett* 2007; 249: 171-177.
- [38] Heinzlbecker J, Kempf KM, Kurz K, Steidler A, Weiss C, Jackson DG, Bolenz C, Haecker A and Trojan L. Lymph vessel density in seminomatous testicular cancer assessed with the specific lymphatic endothelium cell markers D2-40 and LYVE-1: correlation with pathologic parameters and clinical outcome. *Urol Oncol* 2013; 31: 1386-1394.
- [39] Platonova N, Miquel G, Regenfuss B, Taouji S, Cursiefen C, Chevet E and Bikfalvi A. Evidence for the interaction of fibroblast growth factor-2 with the lymphatic endothelial cell marker LYVE-1. *Blood* 2013; 121: 1229-1237.